Proceedings of ASME Turbo Expo 2011
GT2011
June 6-10, 2011, Vancouver, British Columbia, Canada

GT2011-46569

OPTIMIZATION OF A 3-STAGE BOOSTER PART 1: THE AXISYMMETRIC MULTI-DISCIPLINARY OPTIMIZATION APPROACH TO COMPRESSOR DESIGN

Kevin Park *
Mark G. Turner
Kiran Siddappaji
Soumitr Dey
Department of Aerospace Engineering
University of Cincinnati
Cincinnati, OH, USA

Ali Merchant
CADNexus
Burlington, MA, USA

ABSTRACT

In this first part of a two part paper, an axisymmetric multidisciplinary optimization approach for compressors is presented and applied to the design of a three stage booster. The booster has been chosen because its optimization gets little attention in the literature, it has low rotational speed and high curvature, and is also a component with only a few stages to test the capabilities of the approach. Optimization of compressors using a meanline approach have been done in the past, but a meanline code cannot easily deal with complex curvature effects that are accentuated in a booster. An axisymmetric flow solver with a coupled boundary layer and compressor loss models is used for the aerodynamics, and an axisymmetric disk analysis code is used to generate weight-optimum disks for every rotor. The process is driven by the DAKOTA optimization package available from Sandia Labs. A genetic optimizer is used to create the Pareto front for a multi-objective function that includes efficiency, weight, length and number of airfoils. Following the genetic algorithm, a gradient based algorithm is also used. The design space is specified using physical parameters that completely define the multistage compressor. A booster made of titanium is presented in addition to two design studies. One design study explores using carbon-carbon composites and another design study explores restricting the last stage stator to 10 blades to understand if an integrated strut concept is feasible. Several optimum results along the Pareto front are described, and they are not intuitive. The optimizer has found solutions that have very high reactions in the last stage. The near-wall streamlines at the edge of the boundary layer are used as the resulting flowpath for the design. The benefit of the high stage reaction is to keep the rotor at a high tip radius, and have high turning in the following stator with very low diffusion as it matches to a lower radius high pressure compressor. The optimization process is fast enough to replace a meanline approach and explores a large design space to create a novel design.

NOMENCLATURE

a	Speed of sound
C_p	Specific heat at constant pressure
$\dot{m}$	Mass flow rate
M	Mach number
P	Pressure
r	Radial coordinate
R	Ideal gas constant
T	Temperature
V	Velocity

Greek

γ	Ratio of specific heats
λ	(1-blockage) parameter
ρ	Density
θ	Tangential direction
ω	Wheel speed

*Address all correspondence to this author. Email: parkke@mail.uc.edu

Subscripts

le	Leading edge
r	Radial
T	Total
te	Trailing edge
x	Axial

Abbreviations

CAD	Computer Aided Design
3D	Three Dimensional

Introduction

The design of jet engines or gas turbines requires a multi-disciplinary approach. A paper by Turner et al. [1] showed a framework for creating a system built around the engine cycle. This paper is a continuation of that work focussing on the turbomachinery optimization using axisymmetric tools. Part 2 of this paper describes in detail how the resulting axisymmetric solution is used to create an initial 3D design in CAD. This then lays the framework for future 3D optimization.

There have been several recent papers of optimization in turbomachinery. Several papers describe high-fidelity optimization of a single blade row with a single objective function [2–5]. A multidisciplinary approach connected to CAD was presented by Staubach [6]. One paper by Kipouros et al. [7] describes a multi-objective approach for looking at blockage and loss for the optimization of a single blade row.

The current work focusses on optimizing a 3 stage booster using an axisymmetric solver with a coupled boundary layer and an axisymmetric disk code for optimizing the disk for reduced weight. The paper will also explore the optimization using both titanium which is commonly used today for reduced weight or made entirely of carbon-carbon composites. The disk capability has been presented by Gutzwiller [8], Gutzwiller and Turner [9], Gutzwiller et al. [10], and Gutzwiller and Turner [11] explore the use of composites in a transonic fan. A multi-stage axial low pressure compressor or booster is commonly used on multi-spool jet engines, and was chosen as the component of interest due to the difficult design considerations inherent in their design. These difficulties include low rotational speed and high curvature of the flow path. Choosing such a system allows for a challenging multi-objective problem that is difficult to optimize and provides ample opportunity to view design trade-offs in different optima.

Many of the details of this effort including the input and output files used are in a NASA final report by Turner and Dalton [12]. The overall procedure is first described below including the software used, the problem definition, and geometry definition. Following that is a discussion on the optimization process and results.

Software

The main software codes used in this research are:

- T-AXI, an axisymmetric solver for turbomachinery available in its interactive executable form at

  `http://gtsl.ase.uc.edu`
- T-AXI-DISK, an analysis and design tool for supporting disks also available at `http://gtsl.ase.uc.edu`
- DAKOTA (Design Analysis Kit for Optimization and Terascale Applications), available at `http://dakota.sandia.gov/`

T-AXI has been validated using several test cases, and was used as the main turbomachinery analysis code. The loss models used in T-Axi are described by Turner et al. [13]. Essentially the overall entropy rise is calculated for a compressor as a sum of the diffusion loss, shock loss, clearance loss, and endwall loss. An important distinction on using these models in T-AXI when compared to a meanline code is that relatively accurate flow information in terms of Mach numbers, velocities, angles, etc. are available to use as inputs to the loss models.

T-AXI-DISK has been used to analyze and then optimize the supporting disks in order to minimize the mass of the machine. DAKOTA was used as the optimization program and the driver for T-AXI.

Problem Definition

The initial conditions for the low pressure compressor (LPC) were created based on solution values from a cycle analysis carried out in NPSS (a NASA cycle analysis tool for propulsion systems) and are tabulated in Table 1 [14]. These parameters were then used to create the initial geometry files necessary to execute T-AXI using a turbomachinery compressor design code, TCDES, which is a part of the T-AXI suite.

Table 1. Problem Definition

Number of stages	4
$\dot{m}$	92.229 kg/s
Rotation Rate	3538.0 rpm
Overall T_T Rise	90.61 K
Inlet T_T	288.15 K
Inlet P_T	100311.82 Pa
R	0.287 kJ/kg*K

The baseline geometry is shown in Figure 1. The red line indicates the casing, the black line indicates the hub definition, the blue lines indicate blade leading edges, and the green lines indicate blade trailing edges. As only the LPC was to be changed for this project, the first rotor (Fan) definition was locked. In addition, the amount of work done by the fan was kept constant.

Geometry Parameterization

In order to efficiently create and test new geometries, a parameterized model had to be created which allowed the most flexibility in design, and the fewest number of parameters for the optimizer to control. Prior to this effort, work had been done to create the interface between DAKOTA and T-AXI, and between T-AXI and T-AXI-DISK. However, at that point the only geometry that could be varied was the number of blades per blade row.

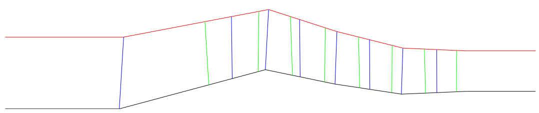

Figure 1. Baseline flowpath and blading.

Work Split The next logical step was to parameterize the amount of work each rotor was required to do. The total amount of work was necessarily kept constant in order to maintain the required pressure rise across the system. The chosen method of parameterization was a cascading system by which a value equal to the percentage of work remaining was assigned to each rotor starting from the fan, and moving to the final rotor. The parameterization may be better understood by examining Table 2.

Table 2. Work Split Example

Rotor No.	Percentage of Work Remaining	Percentage of Total Work
1 (Fan)	50%	50%
2	50%	25%
3	50%	12.5%
4	100%	12.5%
Total	0%	100%

While this approach may seem cumbersome at first, it allows for easier implementation when keeping the total amount of work constant. This is achieved by keeping the sum of the change in angular momentum of the flow constant. That is, $\Sigma \Delta r V_\theta = const.$ for each new design, with the constant determined by the baseline design. As the flow is turned through the engine, it acquires more or less angular momentum. Since work is only done on the flow across the rotors and we are using a free vortex assumption, the sum of the changes in angular momentum may be found by subtracting the rV_θ values at the rotor exits from the rV_θ values at the rotor inlets. In this case, the rV_θ values at the stator exit may be assumed to be equal to the rV_θ value for the inlet of the immediate downstream rotor. This relationship is given explicitly as:

$$\Delta (rV_\theta)_{rotor3} = rV_{\theta rotor3_{te}} - rV_{\theta stator2_{te}} \qquad (1)$$

Hub Definition The flow path geometry of the hub and casing had remained fixed in the work presented by Turner et al. [1]. To extend the capability to a variable flow path and blade geometry required that the actual flow path could be controlled. After careful consideration, the hub was chosen as the controlable surface, with the casing changing based on several other parameters. Several initial parameterizations were explored, but the choice was made to use Bezier curves as the hub definition due to their inherent smoothness and ease of control through control points. The DTNURBS Fortran library was chosen since it was freely available, and there was experience in its use. Figure 2 shows an example spline in green and its control points in red with the locked fan hub in blue. The first control point is coincident with the hub trailing edge of the fan to ensure a continuous hub definition. There is an extra control point colinear with the fan hub and near to the first control point to cause the spline to be tangent to the fan hub at the first control point. This ensures that the entire hub is smooth.

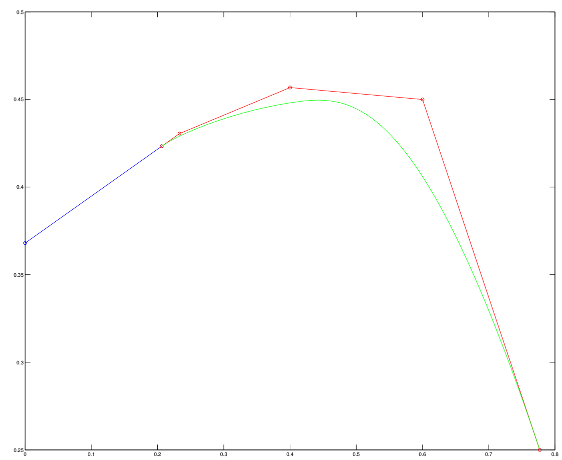

Figure 2. Bezier curve with control points connected to forward straight line section.

The use of Bezier curves enables the construction of very complex, smooth shapes with a small number of parameters. This example uses three (3) points controlled by the optimizer, one of which is colinear, and therefore represents 5 variables. Using an additional control point at the machine exit such that if a line was drawn between the last and second to last control points, that line would be colinear to the engine axis allows for the smooth transition to a purely axial flow path as shown in Figure 3. Figure 3 is meant to demonstrate only the smooth hub. the casing is obviously non-optimal for this case.

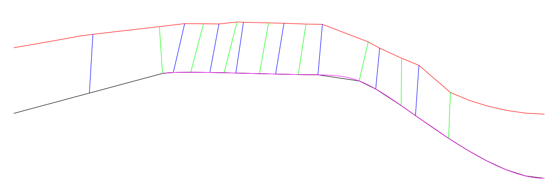

Figure 3. Fully formed hub definition.

Casing Definition The casing definition is a bit more involved. Rather than using a second spline or something similar, the casing is parameterized such that it has the right area to allow the required flow and using other typical turbomachinery parameters such as the axial chord of each row at the hub, the axial taper ratio of each row, the rotor leading edge Mach numbers, the velocity ratios across each rotor, and the axial gaps between rows at the hub and casing. Using the method laid out in the Turbomachinery Compressor Design User Manual [15], the required annular area can be found. From the area and the hub radius, the casing radius can then be calculated. The process is described mathematically below.

The rise in total temperature is calculated across each rotor using Euler's Turbomachinery Equation (2) based on $\Delta\overline{rV_\theta}$ derived from the work split parameters.

$$\Delta T_T = \frac{\omega}{C_p}\Delta\overline{rV_\theta} \tag{2}$$

Using the inlet total conditions and the change in total temperature across each rotor, ΔT_T, the change in total pressure can be calculated using the isentropic flow equation (4).

$$\Delta P_T = P_{T2} - P_{T1} \tag{3}$$

$$\frac{P_{T2}}{P_{T1}} = \left(\frac{T_{T2}}{T_{T1}}\right)^{\dfrac{\gamma}{\gamma-1}} \tag{4}$$

Using these relations, the total temperatures and pressures for each station through the machine may be found. Assigning a Mach Number parameter at the midspan or pitch of each rotor leading edge allows the static temperatures and pressures to be found using the following equations.

$$T = \frac{T_T}{1+\left[\frac{\gamma-1}{2}\right]M^2} \tag{5}$$

$$P = \frac{P_T}{\left(1+\left[\frac{\gamma-1}{2}\right]M^2\right)^{\frac{\gamma}{\gamma-1}}} \tag{6}$$

The basic relations for the speed of sound, Mach number, and density is also be required.

$$a = \sqrt{\gamma R T} \tag{7}$$

$$M = \frac{V}{a} \tag{8}$$

$$\rho = \frac{P}{RT} \tag{9}$$

Using the known information, a set of equations may be constructed to solve for the tip radius of the rotor leading edge. There are four unknown variables: $\bar{r}$, V_x, V_θ, and r_{tip}.

$$A = \frac{\dot{m}}{\rho V_x \lambda} \tag{10}$$

$$A = \pi\left(r_{tip}^2 - r_{hub}^2\right) \tag{11}$$

$$\bar{r} = \frac{r_{hub}+r_{tip}}{2} \tag{12}$$

$$V_x^2 + V_\theta^2 = V^2 \tag{13}$$

$$V_\theta^2 = \frac{\left(\overline{rV_\theta}\right)^2}{\bar{r}^2} \tag{14}$$

Combining and rearranging these equations yields a system of four equations and four unknowns:

$$\pi\left(r_{tip}^2 - r_{hub}^2\right) - \frac{\dot{m}}{\rho V_x \lambda} = 0 \tag{15}$$

$$\frac{r_{hub}+r_{tip}}{2} - \bar{r} = 0 \tag{16}$$

$$V_x^2 + V_\theta^2 - V^2 = 0 \tag{17}$$

$$\frac{\left(\overline{rV_\theta}\right)^2}{\bar{r}^2} - V_\theta^2 = 0 \tag{18}$$

These equations are solved simultaneously and the resulting tip radius is used to create the coordinates for the rotor leading edge and the upstream stator trailing edge. The stator leading edges are solved in the same way, using a new velocity value calculated using the velocity ratio parameter across the upstream rotor. Similarly, the stator leading edge area is equal to the upstream rotor trailing edge area and is used to calculate the upstream rotor trailing edge tip radius.

Axisymmetric Grid

An example of a grid that is created from the hub and casing definitions and used in the axisymmetric solver is shown in Figure 4. The leading and trailing edges of the blade rows are indicated by the green lines.

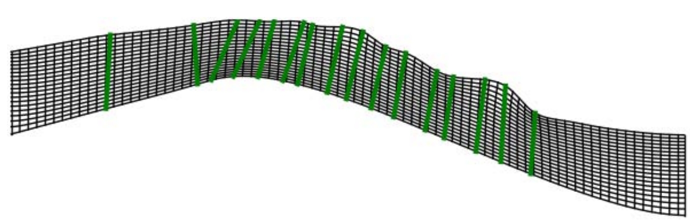

Figure 4. Axisymmetric grid example showing the streamlines calculated by T-Axi and the blade row leading and trailing edge locations in green overlapping the grid.

Disks

There are several parameters which T-AXI forwards to T-AXI-DISK in order to allow it to optimize the disks for a specific design. These parameters include temperature information at the bore and the hub, the ratio of the blade root (firtree) to the blade height, blade density, and several others that are not pertinant to this research. The interface between T-AXI and T-AXI-DISK is built such that the disk for only one blade row at a time is optimized. This allows for inclusion of several schemes to minimize the mass of the complete system. Since T-AXI-DISK allows for the use of multiple materials, two options were devised to find the optimal mass. The first method is simplistic and tests each material individually for every disk, assuming that there is no material change in the machine. Each material is tested for every blade row, and the material that results in the lightest machine is reported. This method could fail to find suitable disks depending on the temperatures and stresses involved depending on the material. The other method assumes there to be a bolted connection between two materials, and attempts to find it. The code automatically accounts for the extra weight that would be incurred at the connection by increasing the blade root/chord ratio. It allows for a range of blade rows to be selected in order to allow flexibility for the user, and a decrease in calculation time. Once again, the best combination of disks is reported back to T-AXI, and the total mass of the machine is recorded.

Optimization

As the goal of this research was to create a tool that could be used to rapidly create unique optimized designs, a suitable optimization method had to be chosen. While gradient-based methods are usually quite rapid in their convergence, their inability to handle discrete design variables like blade counts and their sensitivity to discontinuous design space made them a poor choice for this particular problem. Instead, non-gradient-based optimization methods such as evolutionary algorithms, dividing rectangle schemes, and pattern search methods were considered. Each technique had its advantages and disadvantages, but an evolutionary algorithm proved to be best suited to the discontinuous design space, discrete design variables, and multiple objective functions in this case.

Overview of Evolutionary Algorithms

Evolutionary algorithms (EA), also known as genetic algorithms (GA), use a process analogous to natural selection and evolution in nature. A set of random points is generated in the design space, this is known as the initial population. Each of these design points is evaluated and the results are returned to the algorithm. From this population, the best points are chosen, recombined and mutated in order to create a new set of design points. This process repeats until convergence criteria are met. The basic logic is described below:

1. Create initial population of design points and evaluate them.
2. Select a number of points based on their fitness (natural selection).
3. Apply recombination and mutation to generate new population of design points from selected survivors.
4. Evaluate new design points.
5. Check for convergence. If not converged go to 2.

The specifics of how the points are chosen and how they are then recombined and mutated varies based on the specific algorithm used, but the basic premise remains the same. The specific algorithm used in the optimization is the Multi-Objective Genetic Algoritm (MOGA) from the John Eddy Genetic Algoritm (JEGA) library contained within DAKOTA. This method was chosen for its robust qualities and its suitability for multiple objective functions.

DAKOTA Optimization Loop

Optimization is achieved using an evolutionary algorithm controlled by DAKOTA. Each design point is evaluated using T-AXI-DAKOTA which is executed by DAKOTA using its forking interface. Multiple points are evaluated in parallel, with unique filenames and running directories created to avoid file race conditions. The file flow may be seen in Figure 5. The optimization begins by executing DAKOTA with its input file as an argument. DAKOTA then creates a file containing all the variable information to be evaluated. T-AXI-DAKOTA is called with the input and output file names as arguments. T-AXI-DAKOTA reads the file from DAKOTA and the bootstrap files from the `Setup_Files` directory. It uses the information from the DAKOTA file to create new files, which are modifications of the bootstrap files, in a separate runtime directory and analyzes the case using the T-AXI core. Pertinent response data such as efficiency and mass are returned to DAKOTA via the response file designated at the execution of T-AXI-DAKOTA and the loop is repeated.

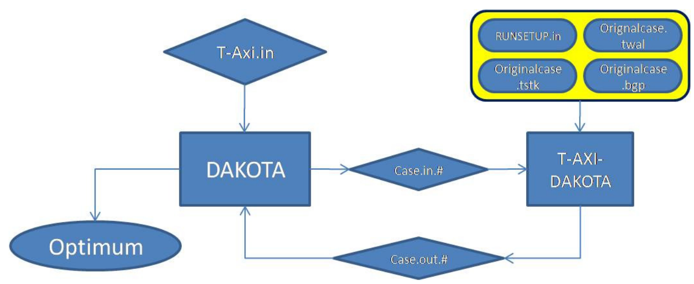

Figure 5. Optimization flowchart.

Optimization Functions, Constraints and Design Parameters

The multi-objective function in the optimization has been set up to minimize the following:

- 1-Efficiency
- Mass
- Length
- Rotor Blade Count
- Stator Blade Count

The constraints on the optimization is the strength of the material for the disk, and that no separation is allowed in the coupled boundary layer. The problem has been defined such that the fan hub has been frozen to demonstrate how the booster can be optimized. This has been done by creating a simple transonic fan with a 1.2 tip Mach number and then creating a "clipped fan" that passes the same flow as the booster. Therefore many of the parameters such as the fan inlet Mach number, fan hub chord or taper ratio are frozen. The restrictions on the geometry are shown in Figure 6. All disks are ring disks for this application including the ”clipped fan” hub. The actual fan disk and blade will be much heavier than the ”clipped fan,” but the difference from design to design would be the same.

For the 3 stage booster plus fan hub, there are 53 design variables, 7 of which are discrete. These variables which have been discussed in the previous sections include:

- Mach entering each rotor (3)
- Velocity ratio across each rotor (3)
- rV_θ exiting stators (3)
- Work split remaining (3)
- Hub spline control points (5, 3 (x,r) points with one colinear)
- Taper ratio of blades (7)
- Axial hub chord (7)
- Hub and tip axial gaps (14)
- Number of blades/row (7, discrete)

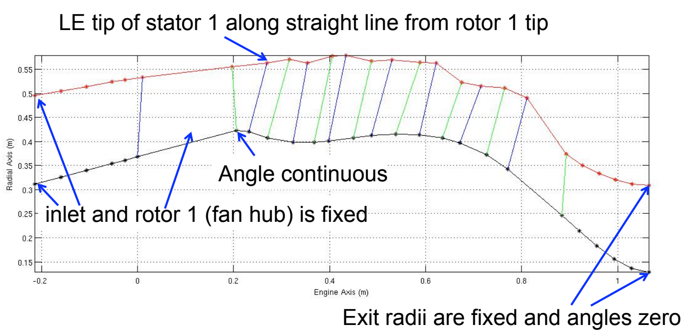

Figure 6. Geometry restrictions of booster design.

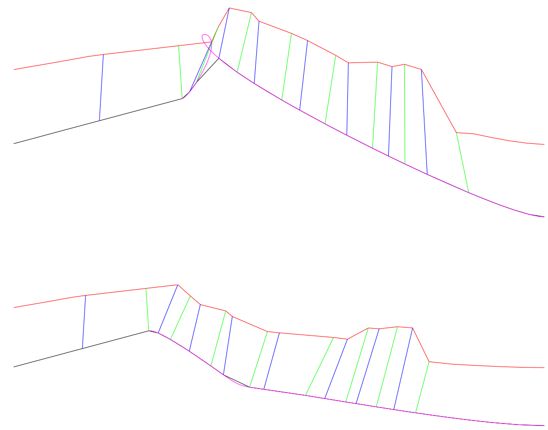

Figure 7. Examples of failed evaluations.

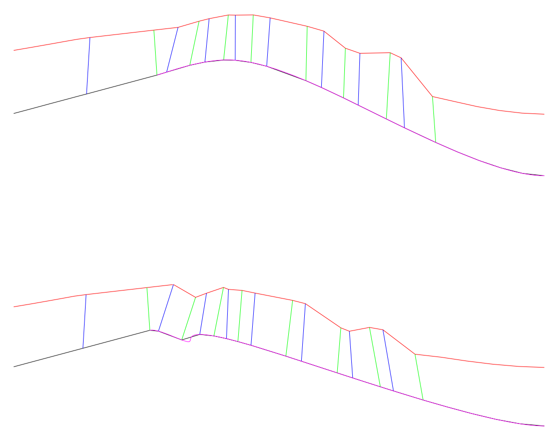

Figure 8. Examples of non-optimal evaluations.

Evaluation Failures

During optimization, designs are often created which T-AXI-DAKOTA is unable to analyze. Two examples are shown in Figure 7. Many times, the T-AXI analysis core is unable to converge the solution, and the evaluation times-out. Other times, due to the bounds on the spline control points, the spline will create a hub shape that loops back on itself (see Figure 7). When T-AXI is unable to find a solution, that design point is reported to DAKOTA as a failure.

Figure 8 show two examples of designs that ran successfully in T-Axi, but are not optimum. The plots in Figures 7-8 only plot the straight line flowpath and the Bezier curve hub. T-Axi takes the hub and casing and fits a cubic spline to it.

System Testing and Verification

Many multiple-objective optimization runs were carried out in order to test the system. The results of one case is detailed here. The objectives for this case were adiabatic efficiency, system mass, machine length, number of stator blades, and number of rotor blades for a total of five objectives. The efficiency was to be maximized and all the other functions minimized. Length was chosen as an objective due to its relation to weight via the shaft. The number of stator and rotor blades were chosen as an objective as a rough way to minimize cost by lowering part counts.

This particular optimization assumed titanium for both the supporting disks and all the blades. The material selection was used to assign material densities and strength in order to create optimum disk designs for each overall system design. The optimization used 30,000 individual design evaluations and was completed in parallel using 4 cores of an Intel I7 processor in approximately 17 hours. The optimization is inherently parallel and can be run on many more processors to reduce the elapsed time.

Figure 9 shows the pareto frontier for adiabatic efficiency and mass. Had this been a more simple two-objective optimization, the frontier would have formed a single curve, rather than the cloud of points seen. This is due to the inclusion of points that are dominated in the efficiency/mass axis, but are non-dominated in the other axes such as efficiency/length (Figure 10) or mass/length (Figure 11). The presentation of the results in this form allows a designer to quickly and easily see multi-dimensional trade-offs and benefits of different designs and apply higher-level knowledge and higher-fidelity tools to refine the machine design.

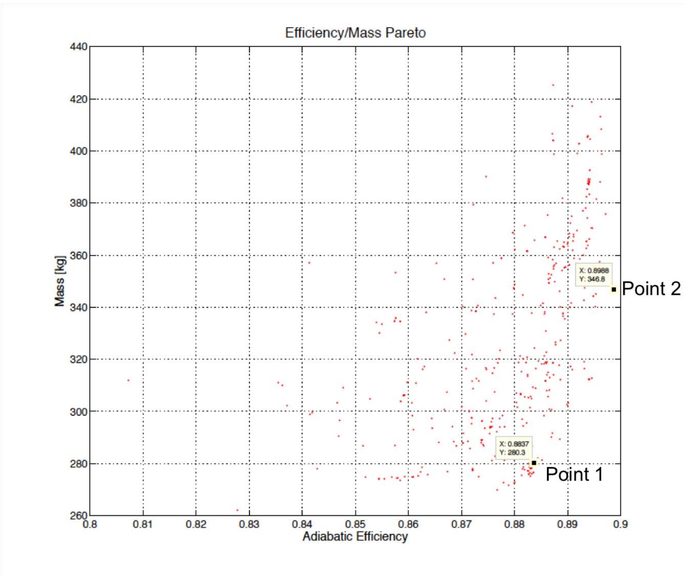

Figure 9. Efficiency/Mass Pareto showing the two selected points for comparison of titanium full optimization.

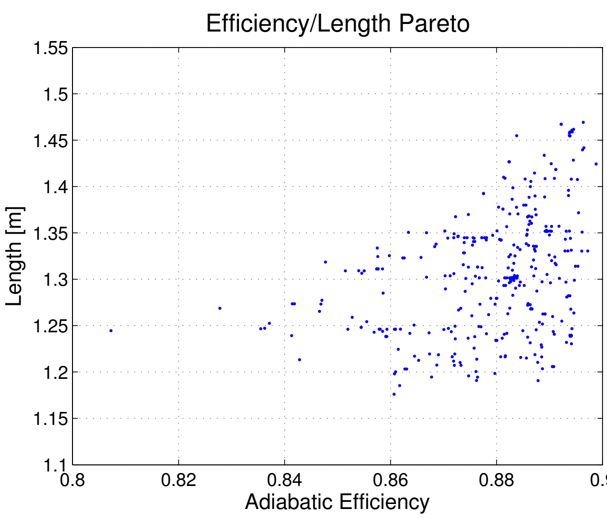

Figure 10. Efficiency/Length Pareto of titanium full optimization.

Gradient-Based Improvements Using the two points from the efficiency/mass pareto as initial points, a gradient-based optimization was performed in an attempt to increase the adiabatic efficiency and validate the genetic algorithm results. The selected points are indicated in Figure 9. Only work split of the three booster rotors and rV_θ of the stators were allowed to be modified by the optimizer in order to keep the flowpath and therefore the mass constant between the two methods. The discrete quantities of blade count were not modified since discrete variables cannot be handled with the gradient-based optimization. Only a single function (1-efficiency) was optimized. There

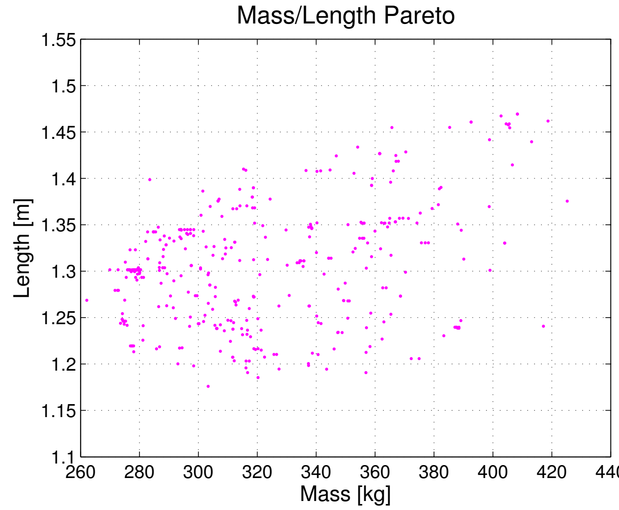

Figure 11. Mass/Length Pareto of titanium full optimization.

was a small improvement in efficiency for both points. Point 1 went from 88.37% to 88.53%, and point 2 went from 89.88% to 90.11%. This demonstrates that the genetic optimization was not fully converged, but would have taken many more iterations to get to this level. The combined method is a hybrid optimization approach, and is an available option within DAKOTA. This manual process has been used to better understand the optimization process.

Composite Design Study

Figure 12 is the efficiency-Mass Pareto for a design study using carbon-carbon composites. The efficiencies are comparable, but the mass is roughly 240 kg less or a 70% weight reduction. This study assumes that there are no manufacturing limitations for the composite, and that they would be rugged enough. The main issue is ruggedness for bird strike or other foreign object damage. This reduction may be worth the development costs associated with the reduction. Because the optimization method automatically calculates the disk mass for the first rotor that is the cropped fan, some of this reduction is for the cropped fan and disk. The study does show a tremendous promise for their use. It also means that efficiency can be optimized since the mass difference is small.

Fixed Stator 4 Blade Count Design Study

While looking at certain feasible design, there were several configurations that had a small number of last stator blades. There is often a strut between the booster and high pressure compressor that supports the fan frame and bearings. There are roughly 10 struts so a design study was run to look at the optimum while holding the number of stator 4 blades to 10. This means there were 52 design variables rather than 53. This concept explores whether the strut could be integrated with turning vanes upstream. Figure 13 is the efficiency-Mass Pareto front for this study. The most efficient point has been chosen to look at in detail.

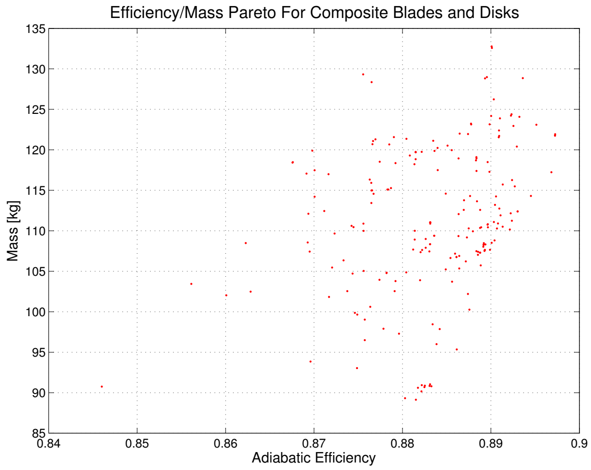

Figure 12. Efficiency/Mass Pareto for the all composite booster optimization.

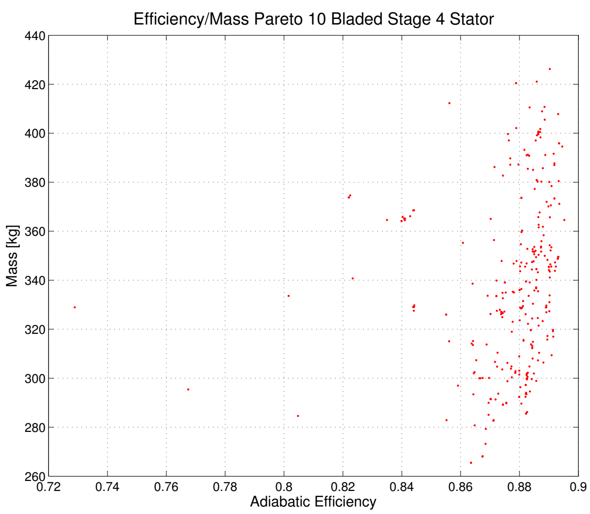

Figure 13. Efficiency/Mass Pareto for the 10 blade Stator 4 optimization.

Discussion of Results

Two points from the titanium optimization pareto (shown in Figure 9) were chosen for closer inspection as well as the most efficient point in the 10 blade Stator 4 optimization. Key parameters are tabulated in Table 3. Figures 14-16 shows the resulting flowpath and blade counts for all the blades for each of these cases respectively. The flowpath plots show the hub and casing endwall splines as well as the displaced streamlines adjacent to the endwall. Because of the constraint, there are no separated points in the boundary layer. The coupled boundary layer is used in T-Axi to account for the blockage of the endwall boundary layers and to give some assessment on the validity of the solution. However it is not truly representative of what is happening in the 3D flowfield. The strategy that will be used is to treat the displaced streamline as the endwall when going to the 3D definition of the blade. This is a naturally smooth curve and may have excellent design features. The wavy wall that these designs are suggesting will be something to explore in 3D, and some average of the flowpath and displaced streamline may yield the best design.

Looking closely at Table 3 one can see what is held fixed in the optimization: the fan work, the fan tip radius, and the stator 4 exit swirl.

The resulting designs are nonintuitive, and the stage reactions are shown in Table 3. The fan and first two stage of the booster reactions are reasonable for a multistage compressor. However the last stage reactions are 1, 0.963, and 0.795, all of which are very high, and might be considered way outside a normal level. The benefit of this large reaction is to keep the tip radius of the rotor as high as possible. The stator then turns the flow to axial but reduces in annular area by coming down in radius to match up with the high pressure compressor IGV.

For the ten stator 4 blade design, it is a bit heavier, and only slightly less efficient (89.52% vs. 90.11%). This may in fact be a better design since it may be integrated with a strut to reduce weight substantially.

The relative work decreases in the downstream stages which makes sense, and each of these designs is plausible.

The choice of design must be made by looking at other merits such as the length and how it is manufactured which has not been addressed by any constraints yet.

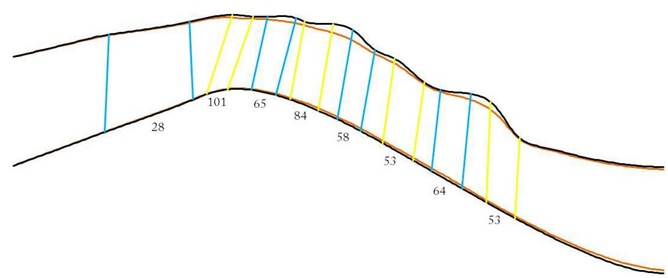

Figure 14. Flowpath of Point 1 Optimization with gradient improvement showing displaced streamlines. Rotors have leading and trailing edges in blue, stators in yellow. The blade count is below the blade row.

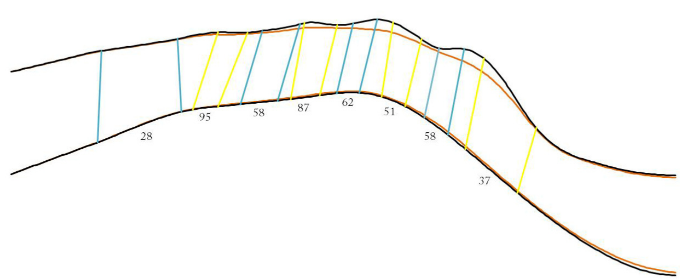

Figure 15. Flowpath of Point 2 Optimization with gradient improvement showing displaced streamlines. Rotors have leading and trailing edges in blue, stators in yellow. The blade count is below the blade row.

Conclusions and Future Work

An axisymmetric multidisciplinary optimization approach for compressors has been presented and demonstrated on a 3 Stage booster application. The parameterization of the design is based on physical quantities and the approach is fast and robust enough to explore an extensive design space. Designs using both titanium and carbon-carbon composite were explored, and weight savings of 70% have been demonstrated using composites. Composites represent a long development item to make sure they are rugged and can be manufactured, but the weight savings would be significant.

In actuality an optimum would be chosen from a Pareto front based on engine requirements such as mission range. For the current optimization, two points have been picked from the Pareto efficiency-mass front that each have good weight and efficiency. The resulting designs are nonintuitive, and each of the designs suggest very high reaction of the last stage and a low aspect ratio last stator. The benefit of this large reaction is to keep the tip radius of the rotor as high as possible. The stator then turns

Table 3. Key Parameters and Attributes for Selected Points

	Point 1 of Overall Opt. Run	Point 2 of Overall Opt. Run	Peak η Point with Ten Stator 4 Blades
Work Fan	40.38%	40.38%	40.38%
Work Rot1	22.09%	26.07%	21.90%
Work Rot2	21.73%	18.47%	20.32%
Work Rot3	15.80%	15.07%	17.39%
Rotors	215	206	208
Stators	291	278	248
Tot. blades	506	476	456
Length [m]	1.301	1.424	1.478
$\eta_{adiabatic}$ booster	88.53%	90.11%	89.52%
Mass [kg]	280.28	346.83	364.61
α_{te} Stator 1_{pitch}	11.356°	9.839°	8.52°
α_{te} Stator 2_{pitch}	3.25°	12.22°	16.03°
α_{te} Stator 3_{pitch}	2.56°	18.15°	7.66°
α_{te} Stator 4_{pitch}	0°	0°	0°
Reaction Fan	0.422	0.435	0.449
Reaction stg2	0.494	0.538	0.589
Reaction stg3	0.603	0.623	0.394
Reaction stg4	1.000	0.963	0.795
Tip M_{rel} Fan	0.856	0.856	0.856
Tip M_{rel} R1	0.646	0.669	0.650
Tip M_{rel} R2	0.605	0.599	0.567
Tip M_{rel} R3	0.632	0.533	0.544

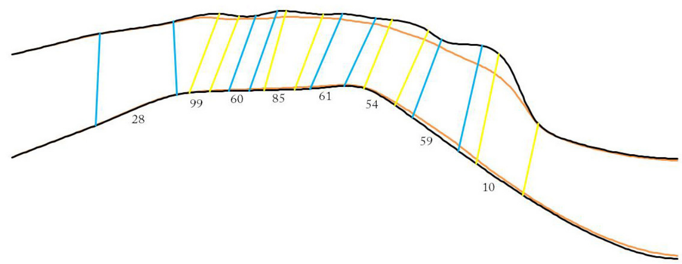

Figure 16. Flowpath of Optimization with Fixing stator 4 with 10 blades showing displaced streamlines. Rotors have leading and trailing edges in blue, stators in yellow. The blade count is below the blade row.

the flow to axial but reduces in annular area by coming down in radius to match up with the high pressure compressor IGV. The resulting casing flowpath comes from the displaced streamline of the axisymmetric solution with coupled boundary layer. This naturally smooth curve may have excellent design features. The optimization process has created a radical design which may lead to improved efficiency designs.

An optimization has also been done with only 10 last stage stator blades to see if a integral stator-strut concept would be viable. The efficiency hit is small, and demonstrates this concept would be useful to explore.

The axisymmetric optimization has many advantages over a meanline approach. It can account for flowpath curvature effects, blade sweep, and endwall diffusion with the coupled boundary layer. It has been demonstrated for a booster which can exacerbate the curvature effects, but is also ideally suited for other compressors and uncooled turbines.

This paper demonstrates some of the potential of the optimization, but its true capability would only be met if more development were done. Medium-term and long-term future work on the Axisymmetric Optimization include:

- Improved monitoring of rapid boundary layer growth and better endwall loss models
- Include all the weights not accounted for including the casing and shaft
- Expand to allow for non-free vortex designs
- Expand to allow for curved leading and trailing edges
- Extend capability to turbines
- Include simple blade stress models to define blade thickness
- Include either constraints or add an objective function for manufacturability including split cases, stacked manufacturing limits on flowpath changes and composite tolerance limits
- Add compressor operability parameters to assess designs with better or worse stall margin
- Have T-Axi work in analysis (off-design) as well as design mode
- Have T-Axi work with gas properties that vary with temperature

ACKNOWLEDGMENT

The authors would like to thank NASA for funding and support through NRA NNC07CB61C - "MDAO of Turbomachinery with Emphasis on Component Optimization".

REFERENCES

[1] Turner, M. G., Park, K., Siddappaji, K., Dey, S., Gutzwiller, D. P., Merchant, A., and Bruna, D., 2010. Framework for multidisciplinary optimization of turbomachinery. Tech. Rep. GT2010-22228, ASME, June.

[2] Pierret, S., Kato, H., Coelho, R. F., and Merchant, A., 2006. "Aero-mechanical optimization method with direct cad access: Application to counter rotating fan design". In GT-2006-90505 ASME Turbo Expo 2006. ASME Paper GT-2006-90585.

[3] den Braembussche, R. A. V., 2008. *Optimization and Computational Fluid Dynamics*. Springer Berlin Heidelberg, January, ch. 6, Numerical Optimization for Advanced Turbomachinery Design, pp. 147–189.

[4] Demeulenaere, A., Purwanto, A., Ligout, A., and Hirsch, C., 2005. "Design and optimization of an industrial pump: Application of genetic algorithms and neural network". *ASME FEDSM2005-77487*, June.

[5] Demeulenaere, A., LigoutI, A., and Hirsch, C., 2004. "Application of multipoint optimization to the design of turbomachinery blades". *ASME GT2004-53110*, June.

[6] Staubach, J. B., 2003. Multidisciplinary design optimization, mdo, the next frontier of cad/cae in the design of aircraft propulsion systems. AIAA Paper 2003-2803, Dayton, OH, July.

[7] Kipouros, T., Jaeggi, D. M., Dawes, W. N., Parks, G. T., Savill, A. M., and Clarkson, P. J., 2008. "Biobjective design optimization for axial compressors using tabu search". *AIAA JOURNAL,* **46**(3), March, pp. 701–711.

[8] Gutzwiller, D. P., 2009. "Automated design, analysis, and optimization of turbomachinery disks". Master's thesis, University of Cincinnati, Cincinnati, OH, September.

[9] Gutzwiller, D. P., and Turner, M. G., 2010. "Rapid low fidelity turbomachinery disk optimization". *Advances in Engineering Software,* **41**(5), May, pp. 779–791.

[10] Gutzwiller, D. P., Turner, M. G., and Downing, M. J., 2009. "Educational software for blade and disk design". ASME Paper Number GT2009-59692.

[11] Gutzwiller, D. P., and Turner, M. G., 2010. Low fidelity turbomachinery disk design studies. Tech. Rep. GT2010-22733, ASME, June.

[12] Turner, M. G., and Dalton, J., 2010. Advanced design techniques for mdao of turbomachinery with emphasis for the engine system. Contract Report NNC07CB61C, NASA Contractor Report from AVETeC, November.

[13] Turner, M. G., Merchant, A., and Bruna, D., 2006. "A turbomachinery design tool for teaching design concepts for axial-flow fans, compressors, and turbines". ASME Paper Number GT2006-90105.

[14] NASA, 2000. *2000 Numerical Propulsion System Simulation Review*. NASA Glenn Research Center, October.

[15] Turner, M. G., Merchant, A., and Bruna, D., 2006. *Turbomachinery Compressor Design User Manual*.